Thermal emission from a metamaterial wire medium slab

G. D'Aguanno,[1,*] N. Mattiucci,[1] A. Alù,[2] C. Argyropoulos,[2] J.V. Foreman,[3] and M.J. Bloemer[3]

[1]*AEgis Tech., Nanogenesis Division 410 Jan Davis Dr, Huntsville, Alabama 35806, USA*
[2]*Dept. of Electrical and Computer Engineering, The University of Texas at Austin, Austin, Texas 78712, USA*
[3]*Dept. of the Army, Charles M. Bowden Facility, Redstone Arsenal, Alabama 35898,USA*
**giuseppe.daguanno@us.army.mil*

Abstract: We investigate thermal emission from a metamaterial wire medium embedded in a dielectric host and highlight two different regimes for efficient emission, respectively characterized by broadband emission near the effective plasma frequency of the metamaterial, and by narrow-band resonant emission at the band-edge in the Bragg scattering regime. We discuss how to control the spectral position and relative strength of these two emission mechanisms by varying the geometrical parameters of the proposed metamaterial and its temperature.

OCIS codes: (160.3918) Metamaterials; (120.6810) Thermal effects; (040.3060) Infrared.

References and links

1. R. Siegel and J. R. Howell, *Thermal Radiation Heat Transfer* (McGraw-Hill, 1981).
2. J.-J. Greffet, R. Carminati, K. Joulain, J.-P. Mulet, S. Mainguy, and Y. Chen, "Coherent emission of light by thermal sources," Nature **416**(6876), 61–64 (2002).
3. J. Le Gall, M. Olivier, and J.-J. Greffet, "Experimental and theoretical study of reflection and coherent thermal emissionby a SiC grating supporting a surface-phonon polariton," Phys. Rev. B **55**(15), 10105–10114 (1997).
4. C.-M. Wang, Y.-C. Chang, M.-W. Tsai, Y.-H. Ye, C.-Y. Chen, Y.-W. Jiang, Y.-T. Chang, S. C. Lee, and D. P. Tsai, "Reflection and emission properties of an infrared emitter," Opt. Express **15**(22), 14673–14678 (2007).
5. G. Biener, N. Dahan, A. Niv, V. Kleiner, and E. Hasman, "Highly coherent thermal emission obtained by plasmonic bandgap structures," Appl. Phys. Lett. **92**(8), 081913 (2008).
6. M. Laroche, R. Carminati, and J.-J. Greffet, "Coherent thermal antenna using a photonic crystal slab," Phys. Rev. Lett. **96**(12), 123903 (2006).
7. X. Liu, T. Tyler, T. Starr, A. F. Starr, N. M. Jokerst, and W. J. Padilla, "Taming the blackbody with infrared metamaterials as selective thermal emitters," Phys. Rev. Lett. **107**(4), 045901 (2011).
8. J. B. Pendry, A. J. Holden, W. J. Stewart, and I. Youngs, "Extremely low frequency plasmons in metallic mesostructures," Phys. Rev. Lett. **76**(25), 4773–4776 (1996).
9. M. Francoeur, S. Basu, and S. J. Petersen, "Electric and magnetic surface polariton mediated near-field radiative heat transfer between metamaterials made of silicon carbide particles," Opt. Express **19**(20), 18774–18788 (2011).
10. S.-A. Biehs, P. Ben-Abdallah, F. S. S. Rosa, K. Joulain, and J.-J. Greffet, "Nanoscale heat flux between nanoporous materials," Opt. Express **19**(S5 Suppl 5), A1088–A1103 (2011).
11. S.-A. Biehs, F. S. S. Rosa, and P. Ben-Abdallah, "Modulation of near-field heat transfer between two gratings," Appl. Phys. Lett. **98**(24), 243102 (2011).
12. S.-A. Biehs, D. Reddig, and M. Holthaus, "Thermal radiation and near-field energy density of thin metallic films," Eur. Phys. J. B **55**(3), 237–251 (2007).
13. P. A. Belov, R. Marques, S. I. Maslovski, I. S. Nefedov, M. Silveirinha, C. R. Simovski, and S. A. Tretyakov, "Strong spatial dispersion in wire media in the very large wavelength limit," Phys. Rev. B **67**(11), 113103 (2003).
14. J.-J. Greffet and M. Nieto-Vesperinas, "Field theory for generalized bidirectional reflectivity: derivation of Helmholtz's reciprocity principle and Kirchhoff's law," J. Opt. Soc. Am. B **15**(10), 2735–2744 (1998).
15. G. D'Aguanno, N. Mattiucci, M. J. Bloemer, D. de Ceglia, M. A. Vincenti, and A. Alù, "Transmission resonances in plasmonic metallic gratings," J. Opt. Soc. Am. B **28**(2), 253–264 (2011).
16. M. A. Ordal, R. J. Bell, R. W. Alexander, Jr., L. L. Long, and M. R. Querry, "Optical properties of fourteen metals in the infrared and far infrared: Al, Co, Cu, Au, Fe, Pb, Mo, Ni, Pd, Pt, Ag, Ti, V, and W," Appl. Opt. **24**(24), 4493–4499 (1985).
17. G. D'Aguanno, M. Centini, M. Scalora, C. Sibilia, Y. Dumeige, P. Vidakovic, J. A. Levenson, M. J. Bloemer, C. M. Bowden, J. W. Haus, and M. Bertolotti, "Photonic band edge effects in finite structures and applications to $\chi^{(2)}$ interactions," Phys. Rev. E Stat. Nonlin. Soft Matter Phys. **64**(1), 016609, 1661–1669 (2001).

1. Introduction

Narrow-band light sources in the mid-infrared (IR) are restricted to light-emitting diodes (LEDs) and quantum cascade lasers, both being characterized by various fabrication challenges, limited efficiency and cost. Thermal light sources have been suggested as viable alternatives in the mid-IR. However, Planck's law [1] dictates their emission to be incoherent and broadband. In the last decade many theoretical and experimental efforts have been dedicated to the possibility of manipulating the black-body emission to realize narrowband mid-IR thermal light sources by using surface waves such as phonon-polaritons in gratings made of polar materials like SiC [2, 3], plasmon-polariton in metallic gratings [4, 5] and leaky surface waves in semiconductor photonic crystals films [6]. Recently, selective thermal emitters based on a metamaterial (MM) perfect absorber have also been demonstrated [7].

The "wire-medium" arguably represents the archetype of a MM. In a seminal paper [8], Pendry and associates showed that a periodic structure made of very thin metallic wires could have an "effective" plasma frequency well below the plasma frequency of the single constituent elements, which is generally in the ultraviolet (UV)-range. The effective plasma frequency could be reduced to near-IR, THz or even GHz range by simply varying the geometry and arrangement of the wires. Heat radiation between metamaterials has been considered in [9], and thermal near-field emission properties in anisotropic materials have been studied in [10-11]. To our knowledge, the thermal emission properties of the MM wire medium have not yet been analyzed, and our study addresses this gap. The geometry analyzed in the current work is consistent with this metamaterial, as schematically represented in Fig. 1, and it is based on a wire medium made of metallic columns with square profile $d \times d$ arranged in a cubic lattice of period Λ, embedded in a generic host medium with electric permittivity ε_b. If we limit our analysis to the special case in which the electric field is entirely parallel to the wires and $\lambda \gg \Lambda$, the effective permittivity of the structure can be written in the form of a lossy, spatially non-dispersive [8], Drude model as:

$$\varepsilon_{eff} = \varepsilon_b \left[1 - \frac{\omega_p^2}{\omega\left(\omega + i\gamma_{eff}\right)} \right] \quad , \quad \gamma_{eff} = \frac{\varepsilon_0}{\sigma} \frac{2\pi c^2}{d^2 \ln\left(\Lambda / d\right)}, \tag{1}$$

where

$$\omega_p = 2\pi c / \lambda_p \quad , \quad \lambda_p = \Lambda \sqrt{2\pi\varepsilon_b \ln\left(\Lambda / d\right)} \ , \tag{2}$$

are the effective plasma frequency and effective plasma wavelength, respectively, σ is the conductivity of the metal. The effective damping term γ_{eff} in (2) not only depends on σ, but also on $1/d^2$ which gives an extra degree of freedom in tailoring the absorption properties of the structure.

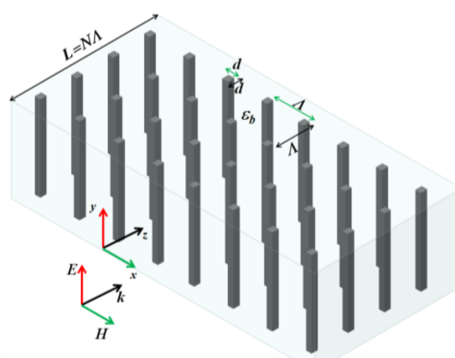

Fig. 1. MM wire medium made of metallic columns of square cross-section $d \times d$ arranged in a cubic lattice of period Λ and embedded in a generic host medium with electric permittivity ε_b. The MM is finite over the z-direction with a thickness $L = N\Lambda$, where N is the number of rows of nanocolumns. We consider a plane, electromagnetic wave at normal incidence with electric field polarized along the wires.

#164725 - $15.00 USD Received 14 Mar 2012; revised 3 Apr 2012; accepted 3 Apr 2012; published 13 Apr 2012

In practice, for the particular polarization analyzed in this work (E-field parallel to the wires), the effective dispersive properties of the metamaterial wire medium become similar to that of a homogeneous metal slab [12]. For a generic polarization of the incident field, this approximation no longer holds and the effects of spatial dispersion become important (as discussed, for example, in [13]). In the following, we analyze the thermal emission properties of this wire medium MM: in Section 2 we detail the main results of our study followed by a discussion and in Section 3 we present our conclusions.

2. Results and discussion

We start our analysis by studying the absorption of the structure under the excitation condition shown in Fig. 1. The absorption $A = 1\text{-}R\text{-}T$, where R is the reflected power (reflectance) and T is the transmitted power (transmittance). According to Kirchoff's law [14], the thermal emissivity is equal to its absorption.

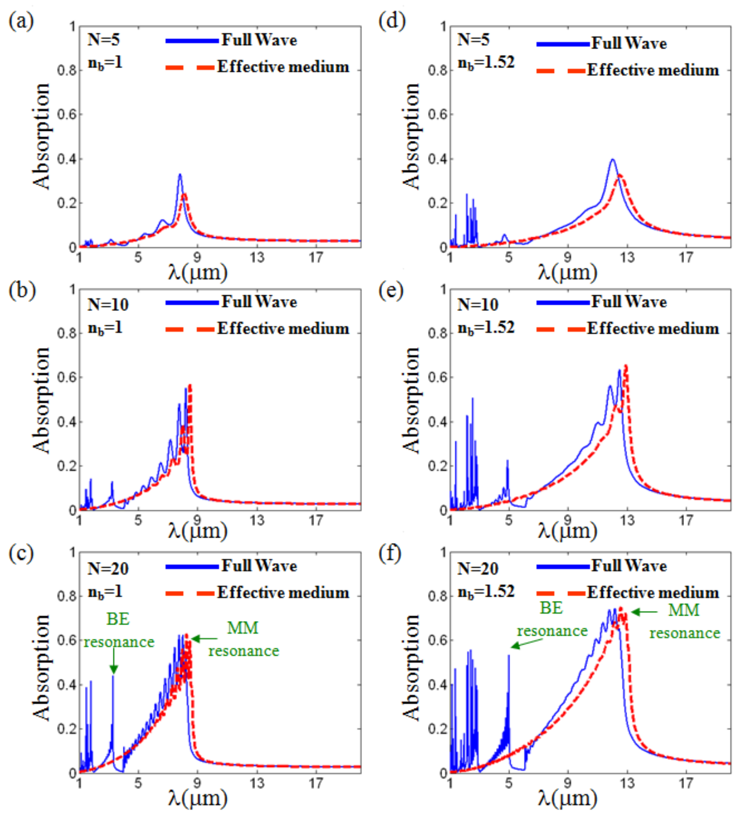

Fig. 2. (Left panel) Absorption vs. incident wavelength for a wire medium MM made of silver nanocolumns with $\Lambda = 2\mu m$, $d = 100nm$ and $\varepsilon_b = 1$ and different number N of rows. Full wave simulations based on the FMM method (continuous line) are compared with analytical results (dashed line) based on Eqs. (1), (2). (Right panel) Same as in the left panel but considering a different host medium with $n_b = \sqrt{\varepsilon_b} = 1.52$.

In Fig. 2 (left panel) we show the absorption of the wire medium immersed in vacuum for N = 5, 10 and 20 rows of nanocolumns, respectively, numerically calculated using the Fourier modal method (FMM) [15]. We compare these results with the analytically calculated absorption of an effective medium, equivalent to a Fabry-Perot etalon, with same length $L = N\Lambda$ and effective parameters given by Eqs. (1), (2). The structure is made of silver nanocolumns with $d = 100nm$ placed in a cubic array of period $\Lambda = 2\mu m$. The dispersion of silver in our calculations is based on experimentally measured data [16] and the silver

#164725 - $15.00 USD Received 14 Mar 2012; revised 3 Apr 2012; accepted 3 Apr 2012; published 13 Apr 2012

conductivity in (1) is $\sigma = 6.28*10^7\ \Omega^{-1}m^{-1}$. Equations (1), (2) predict $\lambda_p \sim 8.7\mu m$. The effective medium model captures with remarkable accuracy the actual behavior of the structure in the homogenization regime, i.e. when $\lambda >> \Lambda$. In addition, Figs. 2(a-c) show how in the Bragg scattering regime $\lambda \sim \Lambda$ a photonic band gap is formed and the wire medium performs even better than the effective medium description in terms of narrow-band absorption features at the band edges for increasing number of periods. It is evident that the effective medium model breaks down near the band edge, since the effective wavelength becomes comparable to the array period and a homogenized model does not hold. In particular in Fig. 2(c), the MM resonance located near the plasma wavelength and the high energy band-edge (BE) resonance in the Bragg scattering regime are indicated. The MM absorption is much broader than the band edge absorption, a clear sign of the different physical mechanisms involved in their formation, as discussed in the following.

In the right panel of Fig. 2, we show the absorption of the same structure, now embedded in a generic, nondispersive host medium with refractive index $n_b = 1.52$. As expected, and in complete agreement with Eqs. (1)-(2), the effective plasma frequency and the corresponding MM resonance are red-shifted to $\lambda_p \sim 1.52*8.7\mu m \sim 13.2\ \mu m$, preserving similar overall resonant features.

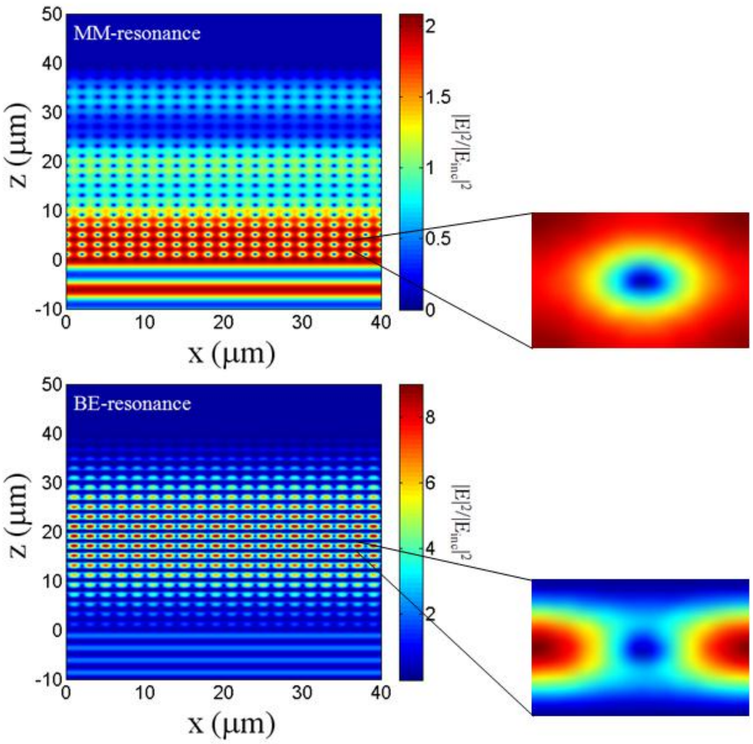

Fig. 3. Cross-sectional view of the electric field localization at the MM resonance and at the BE resonance as indicated in Fig. 2(f). The structure has 20 rows of columns, it starts at $z = 0$ and ends at $z = 40\mu m$. For the help of the eye, the inset shows a magnification of the field localization around a metal column in the two cases.

In Fig. 3, we show the electric field distribution at the MM resonance at $\lambda = 12.2\mu m$ and at the BE resonance at $\lambda = 5.008\mu m$, as indicated in Fig. 2(f). The different field distributions at the two frequencies highlight the different nature of the two resonance regimes. At the MM resonance, a ~20% reflectance is observed and the electric field homogeneously penetrates the structure, being uniformly attenuated along the propagation direction (z-axis), as expected after propagation in a lossy material with low positive refractive index, penetrable to the

#164725 - $15.00 USD Received 14 Mar 2012; revised 3 Apr 2012; accepted 3 Apr 2012; published 13 Apr 2012

impinging wave. This behavior is in complete analogy with the wave propagation in a homogeneous layer of plasmonic material (e.g., silver) at its plasma frequency, except that in the present case the effective plasma frequency of the MM is in the mid-IR, instead of UV. On the contrary, at the BE-resonance the field is strongly localized at the centre of the structure, with a typical single bell-shaped envelope in analogy with the localization properties at the BE resonance in finite, 1-D multilayered structures [17]. In our case the low group velocity and high density of modes available at the BE-resonance [17] not only boosts the local field intensity inside the structure, but at the same time increases the overall absorption over the metallic nanocolumns especially at the high energy band edge where the fields tend to localize more strongly near the metal columns. In both cases, the position of the nanocolumns coincides with the minima of the field, as the field does not penetrate significantly in the metal.

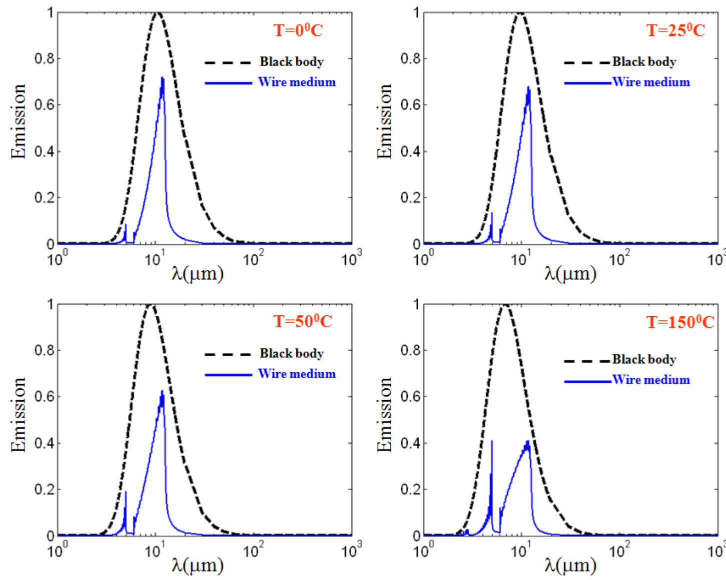

Fig. 4. Normalized emission vs. wavelength for an ideal black body (dashed line) and the wire medium (continuous line) for different temperatures. The peak of the black body emission has been normalized to 1.

In Fig. 4, we show the emission properties of the proposed structure (Fig. 2(f)) compared with the black-body emission at different temperatures. The emission is calculated as the product of the absorption/emissivity A(λ) of the structure multiplied by the Planck distribution of the black-body: $g_{bb}(\lambda) \sim 1/\left\lfloor \lambda^5 \left(e^{hc/K_B T\lambda} - 1\right)\right\rfloor$ [1] with K_B the Boltzmann constant, h the Planck constant, and T the temperature of the source. It is evident that the wire medium can emit quite efficiently both at the MM resonance and at the BE resonance, depending on the temperature of operation. At low temperature, Planck's law favors the emission at the MM resonance, but by increasing the temperature both emissions become accessible. This behavior can simply be explained by considering that the peak of emission of the black-body blue-shifts for increasing temperature. Therefore, the BE resonance, which is located at shorter wavelengths than the MM resonance, will in general be favored for higher temperatures. We remark that this emission pattern can be tuned at will along the entire IR region by simply varying the period Λ and the wire geometry according to Eqs. (1), (2), offering large tunability to tailor the emission properties of the structure in the desired frequency and temperature range.

In order to further increasing absorption, and therefore emissivity, we may for example reduce the wire cross section from *100nm²* to *40nm²*, as shown in Fig. 5. In this case, the absorption at the MM resonance substantially increases, reaching a value >90%. As expected, the effective medium model describes well the behavior of the structure in this long-wavelength regime. Also for this structure the emission at the MM resonance and/or the band edge resonance can be selectively excited depending on the temperature of the structure.

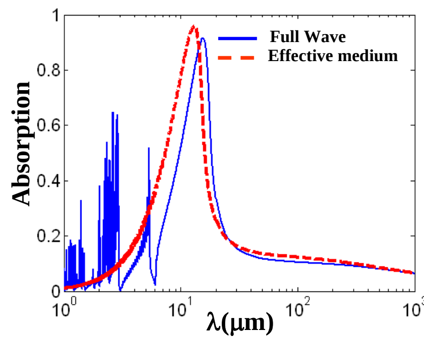

Fig. 5. Absorption vs. incident wavelength for the same wire medium as in Fig. 2(f) except that now the column cross-section is $40\mathrm{nm}^2$.

Although here we have analyzed just the case of the emissivity along the normal, similar emissivity patterns can be obtained at an angle. In this latter case the position of the MM resonance and of the BE resonance will be simply blue-shifted with respect to the normal incidence case.

3. Conclusions

In conclusion, we have studied the thermal emission from a finite metamaterial wire medium composed of silver nanocolumns in a nondispersive dielectric background. We identify two regimes of resonant emission: the first is characterized by broadband emission near the effective plasma frequency of the metamaterial, the second one is characterized by an extremely narrow-band resonance at the band-edge in the Bragg scattering regime. These two resonances can be selectively excited by tuning the temperature of the structure and their spectral position may be tuned along the entire IR region by simply varying the arrangement and size of the wires and/or by varying the refractive index of the host medium. We remark that, although in this work we have considered Ag wires embedded in a dielectric medium, different combinations of metal wires and host media may be similarly explored and analogous results are expected. Moreover, while here we have modeled wires with square cross section, the same results are expected for wires with circular cross section of same area. Finally, we point out that in the present work we have only analyzed the thermal emission properties for E-field parallel to the wires. This condition allows us to consider the metamaterial as an isotropic material with effective dispersion given by Eqs. (1-2), as in the original work [8]. A more complete study to include a generic polarization is beyond the scope of this manuscript and will be left for future investigation.

Acknowledgments

This work has been partially supported by ARO with STTR W31P4Q-11-C-0098,, by DARPA with SBIR W31P4Q-11-C-0109, by the AFOSR YIP award No. FA9550-11-1-0009, and by an ONR MURI No. N00014-10-1-0942.

#164725 - $15.00 USD Received 14 Mar 2012; revised 3 Apr 2012; accepted 3 Apr 2012; published 13 Apr 2012